Ab initio study of yttria-stabilized cubic zirconia surfaces

G. Ballabio,[1,2] M. Bernasconi,[1,2] F. Pietrucci,[2] and S. Serra[1,3]
[1]*Consorzio Corimav, Via Cozzi 53, I-20125 Milano, Italy*
[2]*Dipartimento di Scienza dei Materiali and Istituto Nazionale per la Fisica della Materia, Università di Milano-Bicocca, Via Cozzi 53, I-20125 Milano, Italy*
[3]*Pirelli Labs, Viale Sarca 336, I-20126 Milano, Italy*
(Received 30 April 2004; published 31 August 2004)

First-principles calculations on the main surfaces of yttria-stabilized cubic zirconia of composition $(Y_2O_3)_{0.14}(ZrO_2)_{0.86}$ are presented. While the geometry and surface energy of the neutral (111) and (110) surfaces are comparable with previous results obtained from constrained minimization of the surfaces of pure c-ZrO_2, we have found that on the (100) face the presence of yttrium is crucial to reconcile *ab initio* results with medium-energy ion scattering data. In fact, our simulations suggest that the (1×1) reconstruction of the (100) surface inferred experimentally is stable only in the presence of yttrium segregation at the surface.

DOI: 10.1103/PhysRevB.70.075417 PACS number(s): 68.47.Gh, 68.35.Dv

I. INTRODUCTION

Zirconia (ZrO_2) stabilized in the cubic fluorite phase by the addition of yttria (Y_2O_3) is a fast oxygen conductor for oxygen ions and is the most common solid electrolyte used in solid oxide fuel cells (SOFC) and oxygen sensors.[1] Besides bulk ionic conductivity, the surface properties of yttria-stabilized zirconia (YSZ) are also of importance for the electrochemical applications of this material. For instance, the detailed structural and transport properties of the YSZ surfaces and interfaces with metals are supposed to influence the performances of metal/YSZ composites used as anodes in SOFC.[2] Although a great deal of experimental and theoretical data have been reported for the surface properties of the monoclinic phase of pure ZrO_2 and for tetragonal-stabilized zirconia (at lower yttria content)[3–9] few studies have been devoted to the surface of cubic YSZ.[10–13] For cubic YSZ, experimental structural data are available only for the (100) surface[13] from medium energy ion scattering (MEIS) measurements which suggested a (1×1) reconstruction. Theoretical studies of the structural and electronic properties of pure ZrO_2 surfaces have been performed within density-functional or Hartree-Fock frameworks for the monoclinic and tetragonal phases of pure ZrO_2.[5–9] The surfaces of pure cubic ZrO_2 have been studied as well,[5,14,15] but the local instability of the cubic phase of pure ZrO_2 at low temperature (c-ZrO_2 is stable above 2650 K) prevented to obtain a reliable relaxed surface structure.

In this work we have studied by *ab initio* methods the structure of the main surfaces [(111),(110), and (100)] of a bulk model of YSZ of composition $(Y_2O_3)_{0.14}(ZrO_2)_{0.86}$ that we have generated in a previous work.[16] Yttrium has been reported to segregate at the surface of polycrystalline tetragonal and cubic YSZ.[18–21] However, these results have been challenged by a recent experimental work[22] which reports that yttrium segregation is not significant at the surface of cubic YSZ. Yttrium segregation may indeed depend on the crystalline phase (tetragonal or cubic) and on the particular surface plane as shown in a recent *ab initio* study of the surfaces of tetragonal YSZ.[6] In the cubic phase we have found that yttrium segregation at the (100) surface is necessary to reconcile the optimized *ab initio* geometry with MEIS data. Results on the optimized geometry of the different surfaces are presented in Sec. III after the brief description of the computational details given in Sec. II.

II. COMPUTATIONAL DETAILS

We adopted the density functional theory in the local density approximation (LDA). Ultrasoft[23] and norm-conserving[24] pseudopotentials have been used for oxygen and metal ions, respectively. Semicore states have been included as valence electrons for yttrium and zirconium. Kohn-Sham orbitals have been expanded in plane waves up to a kinetic cutoff of 30 Ry as implemented in the code CPMD.[25] Within the same framework we have previously modeled bulk YSZ. Good comparison with experimental data have been achieved for both structural and electronic properties of bulk YSZ modeled with a cubic supercell containing 92 atoms at composition $(Y_2O_3)_{0.14}(ZrO_2)_{0.86}$ (eight yttrium ions and four oxygen vacancies per supercell).[16] Here, the main surfaces of YSZ have been modeled by cutting the bulk model of Ref. 16 in a slab geometry whose details are given in the next section. The periodically repeated slabs are separated by vacuum 5 Å wide. Brillouin zone integration has been restricted to the Γ-point only of supercells containing up to 138 atoms as described later. Calculations of surface energies have been repeated for both the theoretical lattice constant within the LDA[16] and the experimental lattice parameter ($a=5.1$ Å).[17] Surface relaxation has been obtained by combined simulated annealing via Car-Parrinello molecular dynamics[26] and geometry optimization with the Broyden-Fletcher-Goldfarb-Shanno algorithm.[27] In the Car-Parrinello simulations we used a time step of 0.24 fs and a fictitious electronic mass of 1050 a.u.

The yttrium and oxygen vacancies in the slabs have been initially assigned to their positions in our bulk model.[16] Possible surface segregation of yttrium has been considered for the (100) surface as discussed later. We have considered only stoichiometric surfaces. Recent theoretical calculations on

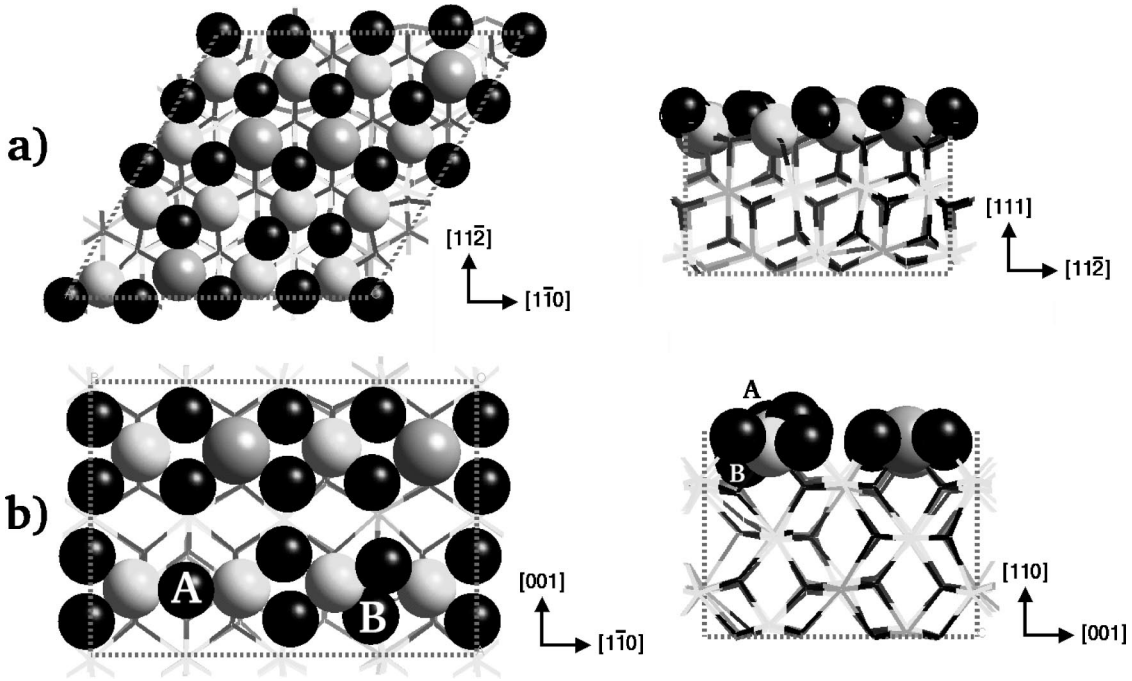

FIG. 1. Geometry of our model of the relaxed (a) (111) and (b) (110) surfaces of YSZ. Large spheres denote surface atoms. Light gray, dark gray and black spheres denote zirconium, yttrium and oxygen ions, respectively. Oxygen atoms labeled A and B in panels (b) are surface atoms nearest neighbor to oxygen vacancies. In the left (right) panels a top (side) view of the two surfaces is reported.

the surfaces of tetragonal YSZ have shown indeed that only stoichiometric surfaces exposing oxygen layers are stable within the feasible range of oxygen chemical potential.[6] Under normal conditions, water is predicted to adsorb dissociatively on the stoichiometric surfaces.[6] Here we consider the clean stoichiometric surfaces relevant for ultrahigh vacuum UHV or dry conditions.

III. RESULTS

A. (111) and (110) surfaces

The (111) and (110) surfaces are neutral and their initial configuration has been chosen as the ideal termination of a bulk supercell obtained by a replication of the 92-atoms supercell of Ref. 16. As discussed in Ref. 16 the oxygen vacancies are distributed in such a way as to be as far as possible from each other (sixth nearest neighbors) and at least next nearest neighbors to yttrium ions. The slab model of the (111) surface contains three metallic layers with an outermost oxygen plane (in the sequence O-Zr-O-O-Zr-O-O-Zr -O) and a total amount of 138 atoms (Fig. 1). One oxygen vacancy out of a total number of six vacancies in the slab is present on each surface of the slab. The surface supercell contains 16 surface unit cells of the ideal pure *c*-ZrO_2. The (111) surface undergoes minor relaxations. The average surface relaxation with respect to the ideal fluorite structure is much smaller than the variance of the deviation from the ideal structure in the bulk. On average, the outermost oxygen (metallic) atoms relax inward (outward) by $\sim$0.01 Å in good agreement with previous calculations on the constrained relaxation of the (111) surface of pure ZrO_2.[14]

The (110) surface is neutral as well. The slab is made of five layers and a total number of 115 atoms. One oxygen vacancy out of a total number of five vacancies in the slab is present on each surface of the slab. The surface supercell

TABLE I. Calculated average vertical relaxation (Å) of the two outermost metallic layers of the (110) surface of YSZ. Relaxations are reported with respect to the ideal truncation of the bulk model of YSZ (YSZ) and with respect to the ideal fluorite structure (fluorite). Previous results of Ref. 14 (from the LDA calculations with the largest *k*-points mesh) on the constrained optimization of the surface of pure *c*-ZrO_2 are also reported. By a positive (negative) sign we refer to an inwards (outwards) displacement with respect to the ideal termination of the bulk.

Surface layer	YSZ	Fluorite	Pure ZrO_2[a]
Zr_1	0.20	0.15	0.184
Zr_2	−0.09	−0.10	−0.164

[a]See Ref. 14.

TABLE II. Surface energies (meV/Å^2) of the relaxed surfaces of YSZ compared with the surface energies of the unrelaxed surfaces of pure *c*-ZrO_2 as given in Ref. 5. The energy of the (100) surface refers to the configuration with yttrium distribution equal to that of the bulk model (see text).

Surface	YSZ	*c*-ZrO_2
(111)	65	74
(110)	90	143
(100)	109	191

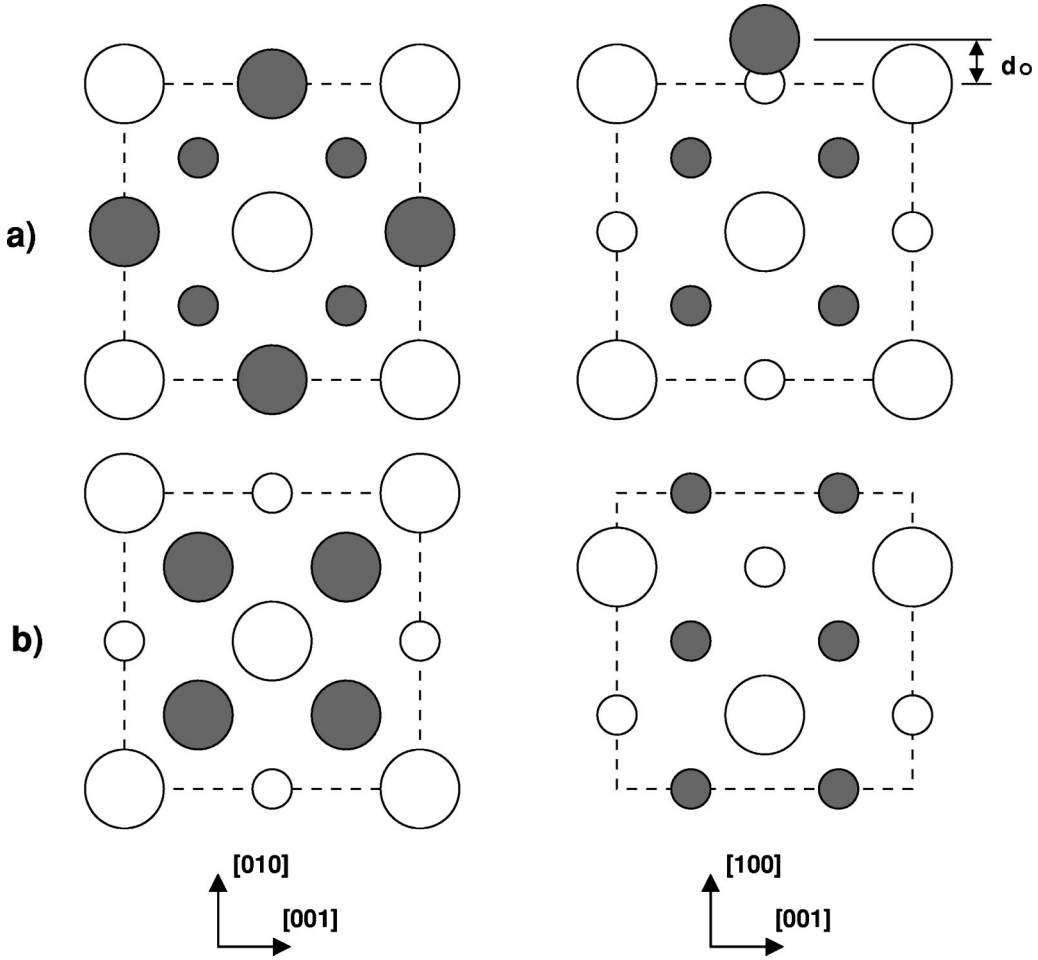

FIG. 2. Top and side views of the YSZ(100) surface in the (a) neutral (1×1) reconstruction proposed experimentally[13] and in (b) charged bulk-like configuration (a full oxygen surface layer is present). d_O denotes the distance between the outermost oxygen and metallic layers. White and black spheres denote metal and oxygen atoms, respectively. Larger spheres are closer to the plane of the figure.

contains eight surface unit cells of the ideal pure c-ZrO_2. The atomic relaxation of the outermost metallic layers are reported in Table I and are similar to those obtained in previous calculations on the constrained relaxation of the (110) surface of pure ZrO_2.[14] Average vertical relaxation of the metal ions with respect to both the ideal fluorite structure and the ideal truncation of the bulk model of YSZ are reported in the table. The oxygen sublattice is strongly distorted with respect to the ideal fluorite structure both at the surface and in the bulk. As a consequence the surface Zr-O plane is buckled, the oxygen atoms on the first layer moving outward by 0.08 Å with respect to the ideal truncation of the YSZ bulk. The average vertical relaxation of the oxygen atoms with respect to the ideal fluorite structure is instead a factor of 2 smaller. However, some surface oxygen atoms which are nearest neighbor to vacancies move much more and up to 0.7 Å, as shown in Fig. 1(b) which reports the relaxed geometry of the (110) surface. Oxygen atom labeled A in the figure was initially nearest neighbor to a vacancy along the $[1\bar{1}0]$ direction. It relaxes in such a way as to align with the metallic row along $[1\bar{1}0]$ and move outwards above the nearest metal ions. Similarly, the oxygen ion labeled B in Fig. 1 is nearest neighbor to an oxygen vacancy in the layer underneath and moves inwards. The surface energies of the relaxed (111) and (110) surfaces are reported in Table II and compared with the results of previous calculations for the unrelaxed surfaces of pure c-ZrO_2.[5] The surface energies in Table I are obtained from slab and bulk calculations at the experimental lattice parameter. Similar calculations at the theoretical lattice parameter provide surface energies which differ by at most 10% with respect to the data in Table II. The (111) face has the lowest surface energy as one would have envisaged by counting the bonds broken by cleavage, or equivalently the change in the coordination number of surface atoms with respect to the their bulk values. The coordination number of Zr and oxygen atoms are, respectively, 8 and 4 in the bulk, 7 and 3 on the (111) surface, 6 and 3 on the (110) surface, and 6 and 2 on the ideal neutralized (100) face [see next section for the structure of the (100) surface].

B. (100) surface

The (100) surface is the only face for which experimental structural data are available. The ideal (100) surface is polar and can be turned into a neutral surface by removing half of the oxygen atoms of the outermost atomic layer. The surface structure emerged from the analysis of MEIS data is reported in Fig. 2(a).[13] The charged surface obtained from the ideal

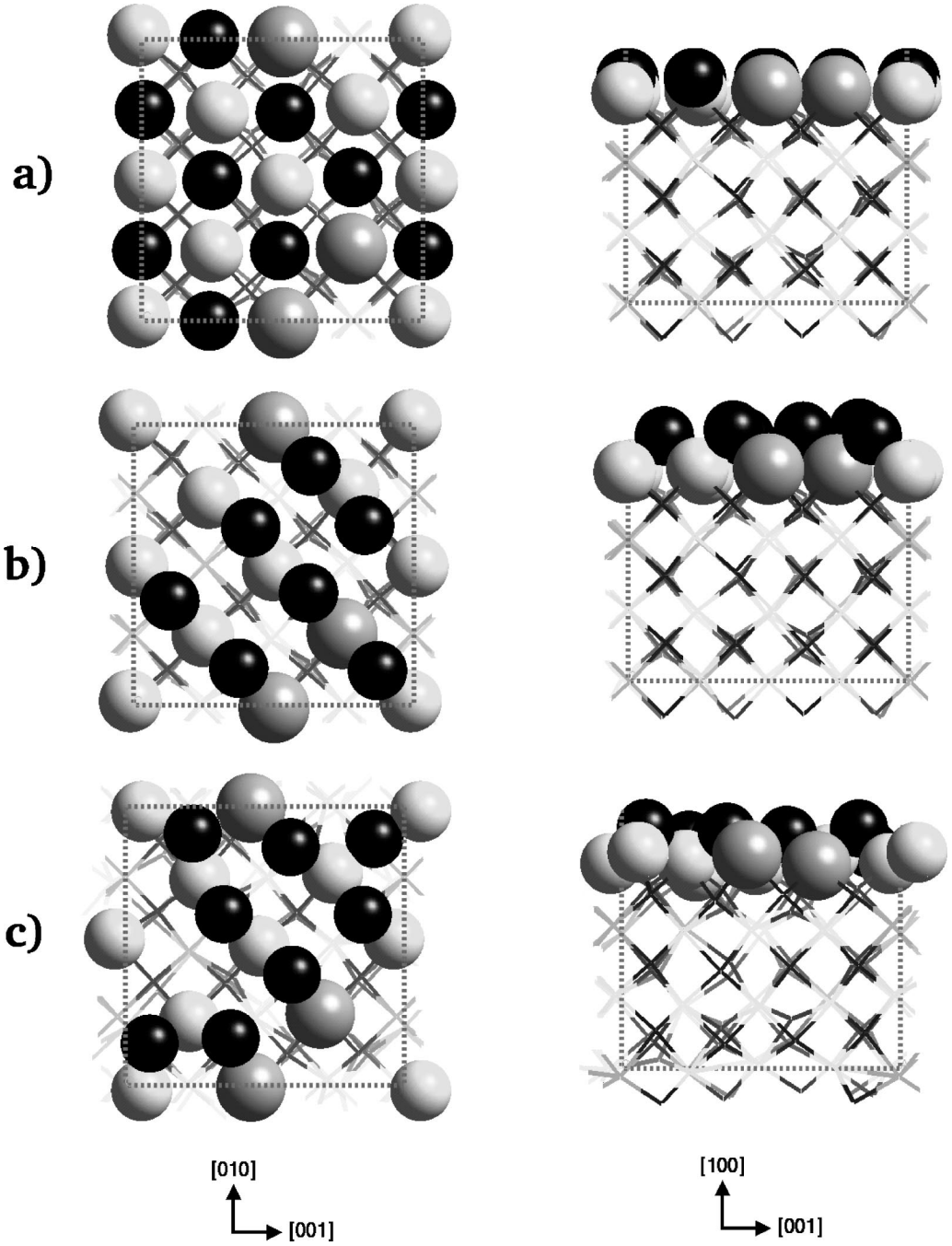

FIG. 3. (a) Reconstructed geometry of the (100) surface proposed experimentally from MEIS data[13] and used as a starting configuration of our simulations. (b) Ideal truncation of the bulk with a row of oxygen ions along the $[01\bar{1}]$ direction. (c) Final configuration obtained by relaxing either the experimental structure in panel (a) or the ideal geometry of panel (b). In the left (right) panels a top (side) view of the slabs are reported. Half of the oxygen atoms are removed from the surface layer to enforce charge neutrality. In the starting geometry of panels (a) and (b), an additional oxygen vacancy is present due to the particular choice of the surface cut of our bulk model of YSZ. In the relaxed configuration of panel (c) the surface vacancy has moved into a bulk oxygen layer. d_O denotes the average distance between the surface oxygen layer and the metallic layer underneath. $d_O = 1.275$ and 0.93 *Å* in panels (b) and (c), respectively. Light gray, dark gray, and black spheres denotes zirconium, yttrium, and oxygen ions, respectively.

termination of the bulk is shown for sake of comparison in Fig. 2(b). To enforce charge neutrality on the ideal termination of the bulk half of the surface oxygen atoms must be removed as shown in Fig. 3(b) for our slab geometry. In this latter geometry, oxygen rows are formed along the [011] direction, but an equivalent configuration could be obtained by aligning the oxygen rows along the perpendicular $[01\bar{1}]$ direction. The structure proposed experimentally reported in Fig. 2(a) and adapted to our slab geometry in Fig. 3(a) corresponds to a (1×1) reconstruction. The oxygen ions of the surface layer move from the tetrahedral sites of the (face-centered-cubic) metallic sublattice of the fluorite structure to

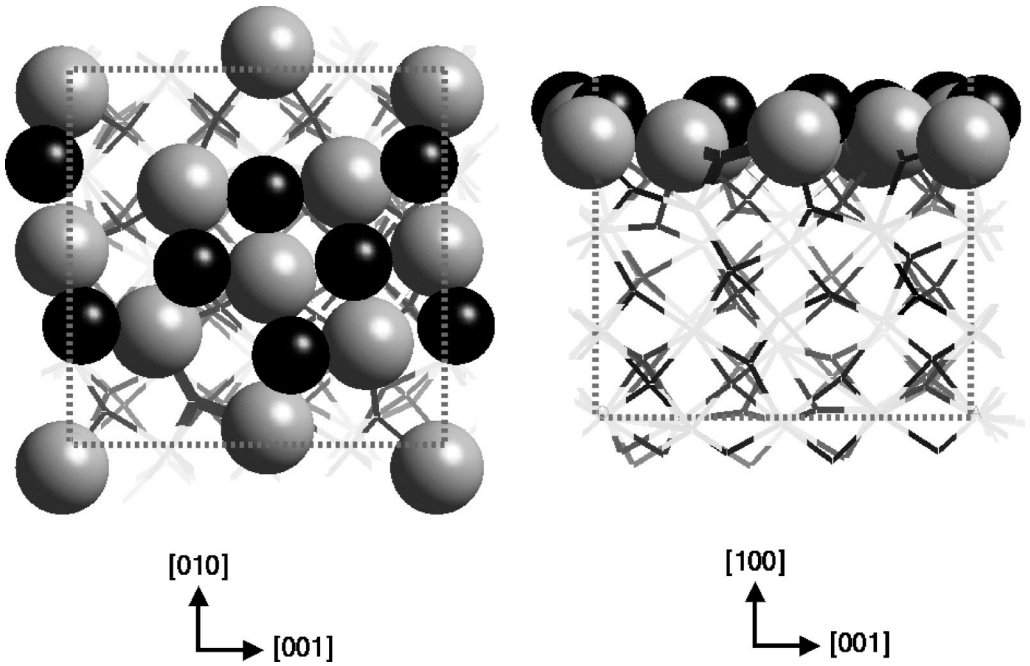

FIG. 4. Reconstructed geometry of the (100) surface with full yttrium segregation at surface. In the left (right) panel a top (side) view of the slab is reported. The color code is the same as in previous figure. Only the outermost oxygen and metal layers are shown in the top view for sake of clarity. Two oxygen vacancies are present on the outermost layer which thus contains six oxygen atoms. In the geometry optimization, obtained via simulated annealing at 500 K, the two outermost layers of the bottom surface of the slab are held fixed.

the octahedral sites. The interplanar distance between the surface oxygen layer and the metallic layer underneath has been assigned to $011(\pm 0.04)\AA$ from MEIS data.[13] On the reconstructed surface the oxygen atoms are coordinated with four metal ions while on the ideal termination of the bulk the oxygen atoms are twofold coordinated. We optimize the surface geometry of our slab either starting from the reconstructed surface proposed experimentally [Fig. 3(a)] or from the neutral ideal termination of the bulk [Fig. 3(b)]. The slab contains nine layers (O-Zr-O-Zr-O-Zr-O-Zr-O) exposing an oxygen layer on both surfaces and a total number of 92 atoms. The surface supercell contains eight surface unit cells of the ideal pure c-ZrO_2. To enforce charge neutrality eight oxygen atoms should be present on each surface of the slab in pure ZrO_2. In our model of YSZ one oxygen vacancy out of a total number of four vacancies in the slab is present on just one surface of the slab which thus contains seven oxygen atoms. The resulting vacancy concentration at surface is close to that inferred experimentally from MEIS data (10%).[13] Surprisingly, we have found that the reconstruction proposed experimentally is unstable and the surface transforms into a structure close to the ideal termination of the bulk but for a disorder in the position of the oxygen ions along both the [011] and $[0\bar{1}1]$ directions [see Fig. 3(c)]. A similar structure is obtained by starting from the ideal termination of the bulk on both sides of the slab. The average d_O parameter is 0.93 Å, smaller than the ideal value for the fluorite structure (1.3 Å) but much larger than the experimental value of 0.11 Å. Moreover, during the simulated annealing we have observed the spontaneous migration of an oxygen vacancy from the surface layer to the oxygen layer underneath. In fact, due to the strong undercoodination of metal ions at the (100) surface, a depletion of oxygen vacancies with respect to the bulk concentration is foreseeable on the ideal geometry of this face. The surface energy of the relaxed (100) surface is given in Table II. The discrepancy with the experimental structural data can be partially overcome by assuming a segregation of yttrium ions at the (100) surface. In fact by moving all the eight yttrium atoms of the slab to the outermost metallic layer (which precisely have eight metallic sites per cell) an oxygen distribution more similar to that of the (1×1) reconstruction proposed experimentally is found to be stable. Figure 4 reports the optimized geometry of the yttrium-rich (100) surface obtained by starting from oxygen atoms in the ideal tetrahedral sites. The presence of the yttrium monolayer induces large strains in the structure which relaxes via diffusion of few vacancies. As a result two oxygen vacancies are present on the relaxed uppermost yttrium-rich surface of the slab (see Fig. 4). The oxygen atoms on the second layer nearest neighbors to the surface vacancies move upwards and are 0.55 $\AA$ below the surface metallic plane. Although strongly distorted, the (1×1) reconstruction proposed experimentally with oxygen atoms in the octahedral sites is clearly recognizable in Fig. 4. The oxygen atoms close to the octahedral sites move inwards lying very close to the underlying metallic layer. On average, the d_O parameter is 0.59 Å, still larger than the experimental value of 0.11 Å inferred from MEIS data.[13] One may envisage that the real surface might be formed by patches of the yttrium-rich configuration in Fig. 4 and of the yttrium-poor geometry of Fig. 3(c). The picture that emerges from the simulations suggests that the geometry of the (100) surface of YSZ is much more disordered and distorted with respect to the (average) ordered structure proposed experimentally[13] which might be responsible for the anomalously low surface

Debye temperature assigned experimentally to fit MEIS data with the structural model of Fig. 2(a).

IV. CONCLUSIONS

In summary we have studied the main surfaces of yttria-stabilized cubic zirconia by first-principles calculations. The geometry and surface energy of the neutral (111) and (110) surfaces are comparable with previous results obtained from constrained minimization of the surfaces of pure c-ZrO_2.[14] On the contrary on the (100) face which requires a surface rearrangement to enforce charge neutrality we have found that the presence of yttrium is crucial to reconcile *ab initio* results with MEIS measurements[13] which are the only experimental structural data available on the surfaces of cubic YSZ. In fact, our results suggest that the (1×1) reconstruction of the (100) surface inferred experimentally from MEIS data is stable only in the presence of yttrium segregation at surface. Thus, the comparison between theoretical and experimental structural data provides an indirect evidence of the still debated segregation of yttrium at the (100) surface of YSZ.[18–22]

[1] B. C. H. Steele, J. Power Sources **49**, 1 (1994).
[2] S. P. Jiang and S. P.S. Badwal, Solid State Ionics **123**, 209 (1999).
[3] K. Meinel, K.-M. Schindler, and H. Neddermeyer, Surf. Sci. **532–535**, 420 (2003).
[4] V. Maurice, M. Salmeron, and G. A. Somorjai, Surf. Sci. **237**, 116 (1990).
[5] A. Christensen and E. A. Carter, Phys. Rev. B **58**, 8050 (1998).
[6] A. Eichler and G. Kresse, Phys. Rev. B **69**, 045402 (2004).
[7] F. Hasse and J. Sauer, J. Am. Chem. Soc. **120**, 13503 (1998).
[8] A. Hoffman, S. J. Clark, M. Oppen, and I. Hahndorf, Phys. Chem. Chem. Phys. **4**, 3500 (2002).
[9] R. Orlando, C. Pisani, E. Ruiz, and P. Sautet, Surf. Sci. **275**, 482 (1992).
[10] J. Nowotny, M. Sloma, and W. Weppner, Solid State Ionics **28–30**, 1445 (1988).
[11] F. Parmigiani, L. E. Deperp, L. Sangaletti, and G. Samoggia, J. Electron Spectrosc. Relat. Phenom. **63**, 1 (1993).
[12] W. C. Simpson, W. K. Wang, J. A. Yarmoff, and T. M. Orlano, Surf. Sci. **423**, 225 (1999).
[13] T. Nishimura, H. Toi, Y. Hoshino, E. Toyoda, and Y. Kido, Phys. Rev. B **64**, 073404 (2001).
[14] M. Alfredsson and C. R. A. Catlow, Phys. Chem. Chem. Phys. **3**, 4129 (2001).
[15] S. Gennard, F. Corà, and C. R. A. Catlow, J. Phys. Chem. B **103**, 10158 (1999).
[16] G. Stapper, M. Bernasconi, N. Nicoloso, and M. Parrinello, Phys. Rev. B **59**, 797 (1999).
[17] C. Pascual and P. Durán, J. Am. Ceram. Soc. **66**, 22 (1983).
[18] A. J. A. Winnubst, P. J. M. Kroot, and A. J. Burggraaf, J. Phys. Chem. Solids **44**, 955 (1983).
[19] J. S. Solomon and J. T. Grant, J. Vac. Sci. Technol. A **3**, 373 (1985).
[20] D. Majumdar and D. Chatterjee, Thin Solid Films **206**, 349 (1991).
[21] M. Cotter and R. G. Egdell, J. Solid State Chem. **66**, 364 (1987).
[22] A. Bernasik, K. Kowalski, and A. Sadowski, J. Phys. Chem. Solids **63**, 233 (2002).
[23] D. Vanderbilt, Phys. Rev. B **41**, 7892 (1990).
[24] N. Troullier and J. Martins, Phys. Rev. B **43**, 1993 (1991).
[25] CPMD V3.7, Copyright IBM Corp 1990–2001 and Copyright MPI fuer Festkoerperforschung Stuttgart 1997–2001.
[26] R. Car and M. Parrinello, Phys. Rev. Lett. **55**, 2471 (1985).
[27] W. H. Press, S. A. Teukolsky, W. T. Vetterling, and B. P. Flannery, *Numerical Recipes* (Cambridge University Press, Cambridge, 1992).